



HAL
open science

The influence of stresses on ageing kinetics of 3Y- and 4Y- stabilized zirconia

Chong Wei, Laurent Gremillard

► **To cite this version:**

Chong Wei, Laurent Gremillard. The influence of stresses on ageing kinetics of 3Y- and 4Y- stabilized zirconia. *Journal of the European Ceramic Society*, 2018, 38 (2), pp.753-760. 10.1016/j.jeurceramsoc.2017.09.044 . hal-01758659

HAL Id: hal-01758659

<https://hal.science/hal-01758659>

Submitted on 6 Mar 2019

HAL is a multi-disciplinary open access archive for the deposit and dissemination of scientific research documents, whether they are published or not. The documents may come from teaching and research institutions in France or abroad, or from public or private research centers.

L'archive ouverte pluridisciplinaire **HAL**, est destinée au dépôt et à la diffusion de documents scientifiques de niveau recherche, publiés ou non, émanant des établissements d'enseignement et de recherche français ou étrangers, des laboratoires publics ou privés.

The influence of stresses on ageing kinetics of 3Y- and 4Y- stabilized zirconia

Published in: Journal of the European Ceramic Society, 2018, 38 (2), pp. 753-60,
<https://doi.org/10.1016/j.jeurceramsoc.2017.09.044>

C. Wei, L. Gremillard
Univ. Lyon, INSA-Lyon, CNRS, MATEIS, UMR 5510, F-69100 Villeurbanne, France

Abstract

Hydrothermal ageing is one of the most important limiting factors for the use of yttria-stabilized zirconia ceramics in contact with water-containing environments. It consists in the transformation of tetragonal phase to monoclinic phase, initiates on the surface of zirconia in the presence of water, and leads to roughening and potentially to micro-cracking and loss of integrity. The present work seeks to explore the influence of applied and residual mechanical stresses on the ageing kinetics of 3Y- and 4Y-TZP. Residual stresses were obtained by rough polishing. A subsequent Annealing step was employed for the preparation of samples free of residual stresses. All samples were submitted to *in situ* 3-points bending tests in water vapour atmosphere inside an autoclave at 134°C, allowing surfaces with a mechanical stress gradient to be exposed to hydrothermal ageing. The evolution of the monoclinic fraction with time and stress was then analysed using Mehl-Avrami-Johnson equation.

Introduction

Since the failure events of Prozyr® femoral heads in 2001–2002 occurred, the studies of the ageing behavior of zirconia ceramics has become the topic of many works. Hydrothermal ageing (also called LTD for Low Temperature Degradation) is a low temperature tetragonal-to-monoclinic phase transformation ($t \rightarrow m$) that occurs on the surface of zirconia ceramics in humid environment. This ageing process is strongly influenced by microstructural parameters (such as stabilizer nature and content, density, surface finish, grain size, cubic phase content, etc.) and mechanical stresses. This work focuses on the influence of both applied and residual stresses on the hydrothermal ageing behavior, which is not yet completely understood [1]. Schmauder and Schubert [2] showed that hydrothermal ageing does not occur in stress-free grains of zirconia, but starts at the surface of Y-TZP in the presence of water vapor and stresses. It is explained by Schubert and Frey [3] that when the water radicals penetrate into the oxygen vacancy present in the zirconia lattice, a lattice contraction occurs, causing tensile micro-stresses that lead to nucleation of the phase transformation. On the contrary, using DFT studies, Gebressilassie showed that the penetration of water in the zirconia lattice does not lead to lattice contraction, but rather to decrease of the energy barrier for the t - m transformation [4]. Both these studies hint to an influence of stresses on hydrothermal ageing, either directly [2] or through energetic considerations [4]. Indeed, Li et al. showed that a small applied tensile stress accelerates the ageing process of zirconia and a compressive stress has little effect on the degradation in hot water (97°C) [5]. However Lughì et Sergo [6] indicated that tensile stresses of the order of some hundreds MPa are sufficient to promote LTD. Deville [7] indicated that the ageing sensitivity of zirconia is directly linked to the type (compressive or tensile) and amount of residual stresses.

The present work seeks to relate the presence of residual and applied stresses to the ageing process of different zirconia ceramics (3Y and 4Y-TZP). In particular, since ageing proceeds by a nucleation and growth mechanism [8-11], the ageing kinetics are currently described using a Mehl-Avrami-Johnson (MAJ) equation. Previous works could relate some parameters of the MAJ equation to the nucleation rate and growth rate of the monoclinic phase [10, 11]. Thus by observing changes on these parameters, the present work will also seek to determine how the presence of mechanical stresses can influence the nucleation and growth rates.

2. Materials and methods

2.1. Material preparation

The experimental flowchart is summarized in figure 1. The samples were fabricated starting from three different ultra-pure Y-TZP powders (TZ3YS, TZ3YE, TZ4YS, Tosoh, Japan). TZ3YS and TZ3YE contain 3 mol.% yttria (in addition, TZ3YE contains 0.25 wt.% Al₂O₃). TZ4YS contains 4 mol.% yttria. The zirconia green bodies used in the present study were prepared by slip casting. The slurries were prepared by mixing the powders in water (70 wt.% solid content) using Darvan 821A as a dispersing agent (1.2 wt.% as compared to the weight of powder), and ball-milling with 3Y-TZP balls for 24 hours. They were then cast in a plaster mold, left to dry first in the mold for 24 hours then in air for at least one week. After drying, the cast green bodies were sintered in a programmable electrical furnace (sintering conditions chosen from previous experience to reach full density: debinding at 550 °C for 5h (heating rate 1°C/min); sintering at 1430°C for 5 h (heating and cooling rate 5°C/min)). The sintered samples were ground in the shape of plates (1.2×20×60 mm for $\sigma_{\max} \leq 300\text{MPa}$, 1.2×20×25 mm for $\sigma_{\max} > 300\text{MPa}$) and polished (using diamond abrasive decreasing in size down to 1 μm). The polishing procedure ensured the removal of all microcracks induced by grinding, but was conducted so that the residual stresses induced by grinding were not completely removed. Finally, half of the polished samples were annealed (1250°C for 0.5h at heating rate of 5°C/min according to a published procedure [12,13]) in order to remove residual stresses. This procedure ensured that all samples (polished and polished + annealed) presented similar roughness and a surface free of microcracks. The “polished only” samples will be labelled xYzP, where x is 3 or 4 (mol% of yttria) and z is E or S (nature of the powder), while the annealed samples will be labelled xYzA, as shown in Table 1.

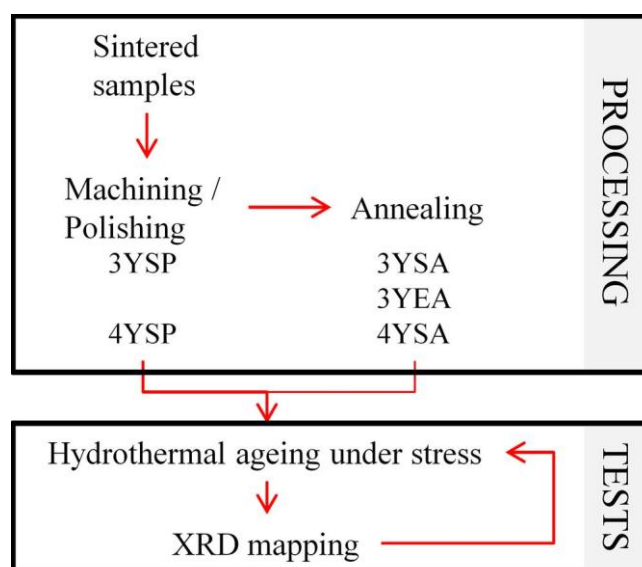


Figure 1: Experimental flow chart

Table 1: Samples prepared for the study of applied stress

	Polished sample	Annealed sample
σ_{max} (MPa)	100	100, 300, 350 and 600
TZ3Y-S	3YSP	3YSA
TZ3Y-E		3YEA
TZ4Y-S	4YSP	4YSA

2.2. Bending test

This study uses three-points bending test to apply a stress gradient on the zirconia plates. Dedicated sample holders were designed, able to perform 3-points bending tests under constant load inside an autoclave (Fig.2). The positioning accuracy of the sample in the sample holder is estimated to ± 1 mm. The load is applied manually through a screw, while the deflection is measured by an external LVDT sensor until the desired deflection is reached. The desired deflection is calculated after the desired maximum applied stress (σ_{max} , between 100 and 600 MPa) using the following equation:

$$\sigma_{max} = E\varepsilon = \frac{6E\delta h}{l^2} \quad (1)$$

Where σ_{max} is maximum stress of sample surface, E is flexural modulus of elasticity (200 GPa), ε is the maximum strain in the outer surface, δ is the deflection, h is the sample thickness, and l is distance between external rollers (50 mm for σ_{max} up to 300 MPa, 20 mm for σ_{max} 350 or 600 MPa).

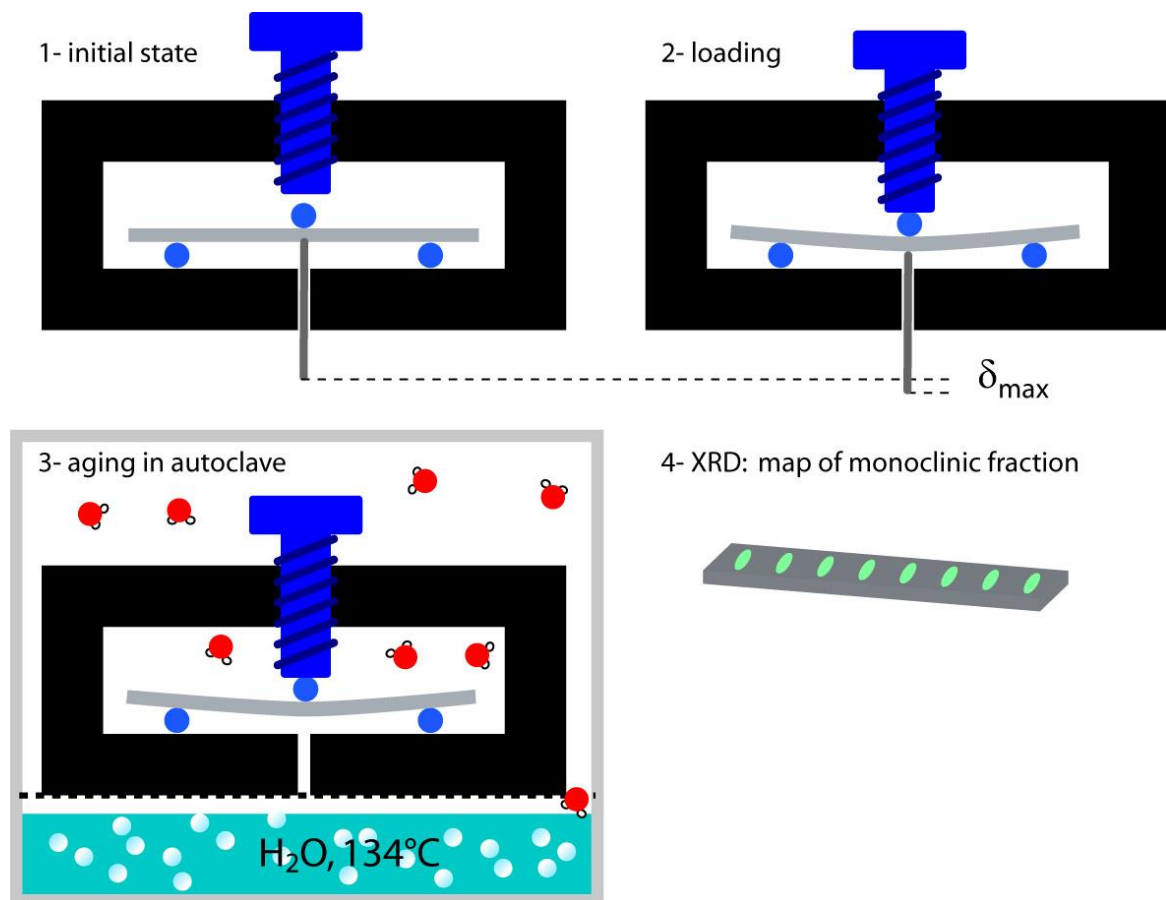


Figure 2: Experimental process for the study of applied stress

The upper surface was in compression, the lower one in tension. The applied stress decreased linearly from $\pm \sigma_{\max}$ (in the center of the plate, under the central roller) to 0 (under the external rollers and further). Finally the stress distribution of each side of the sample under bending test is visualized in Fig. 3.

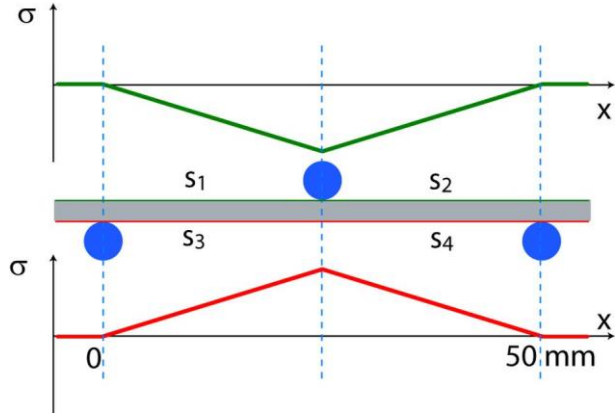


Figure 3: Applied stress distribution of every side of the sample under bending test

2.3 Microstructures and residual stresses

The residual stresses were quantified by x-ray diffraction (XRD, D8 advance Diffractometer (Bruker, Germany) with $K\alpha$ radiations, in Bragg-Brentano configuration), associated with Rietveld refinement (Topas 4.0 software, Bruker, Germany). Rietveld refinement was conducted with the fundamental parameters approach. This allowed both the quantification of the different phases, the determination of their lattice parameters (from which the yttrium amount inside each phase was determined using Scott's calibration curves [14]), and the determination of crystallite size (parameter CrySize_L) and residual microstress σ_{μ} (calculated as: $\sigma_{\mu} = \frac{\pi \times E \times \text{strain}_G}{360}$, with E the Young modulus (taken here at 200 GPa)). Note that the crystallite size measure that way is the size of the diffracting (crystallographically coherent) domains, and may be much smaller than the grain size observed by SEM.

2.4 Assessment of the ageing kinetics

Every few hours, the samples were removed from the autoclave and unloaded. Then a cartography of the amount monoclinic phase was obtained by X-ray diffraction: the samples were mounted on an X-Y-Z moving stage, their long axis along the X axis. XRD measurements were performed every 2 mm along the X axis (at constant and adequate Y and Z), to get a determination of the monoclinic fraction versus position, thus versus applied load during ageing. To get a high enough signal/noise ratio, the width of the analyzed area was around 5 mm, preventing the detection of rapid changes. XRD patterns were recorded in the $27\text{-}33^\circ$ (2θ) range with a scan speed of 0.2 min^{-1} and a step size of 0.05° . The monoclinic ZrO_2 phase content (V_m) was expressed after Toraya's equation [15]:

$$V_m = \frac{1.311X_m}{1 + 0.311X_m} \quad (2)$$

In which the value of X_m was calculated using Garvie and Nicholson method [16]:

$$X_m = \frac{I_m^{-111} + I_m^{111}}{I_m^{-111} + I_m^{111} + I_t^{101}} \quad (3)$$

Where I_p^{hkl} is the area of the diffraction peak related to the (hkl) plane of phase p (m for monoclinic and t for tetragonal).

For each sample, the knowledge of V_m versus time and stress allowed plotting ageing kinetics at different stress levels, further analyzed using the MAJ formalism.

3. Results

3.1 Determination of residual stresses

Fig. 4 shows details of the XRD measurements conducted on 3YSA, 3YSP, 4YSA and 4YSP samples. Only tetragonal and cubic phases were detected in the annealed samples. The XRD diagrams of the polished samples showed two main differences with the ones for annealed samples: apparition of monoclinic phase, and distortion of the highest peaks (shoulder indicated by an arrow at the left of the main peaks), which was interpreted as the presence of a distorted tetragonal phase [13] (no fit by orthorhombic phase was possible on these peaks). Unfortunately the angular resolution is not high enough to separate clearly the different convoluted peaks, thus to fit with absolute certainty the cubic and distorted tetragonal phases, but it seems the amount of cubic phase remains constant after annealing (~24% for 3YS, ~43% for 4YS), while cubic phase gets slightly less distorted (lower second order strains after annealing). The distorted tetragonal phase presents lattice parameters between 1 and 2% larger than the tetragonal phase. An accurate analysis of its crystallite size and microstress is impossible.

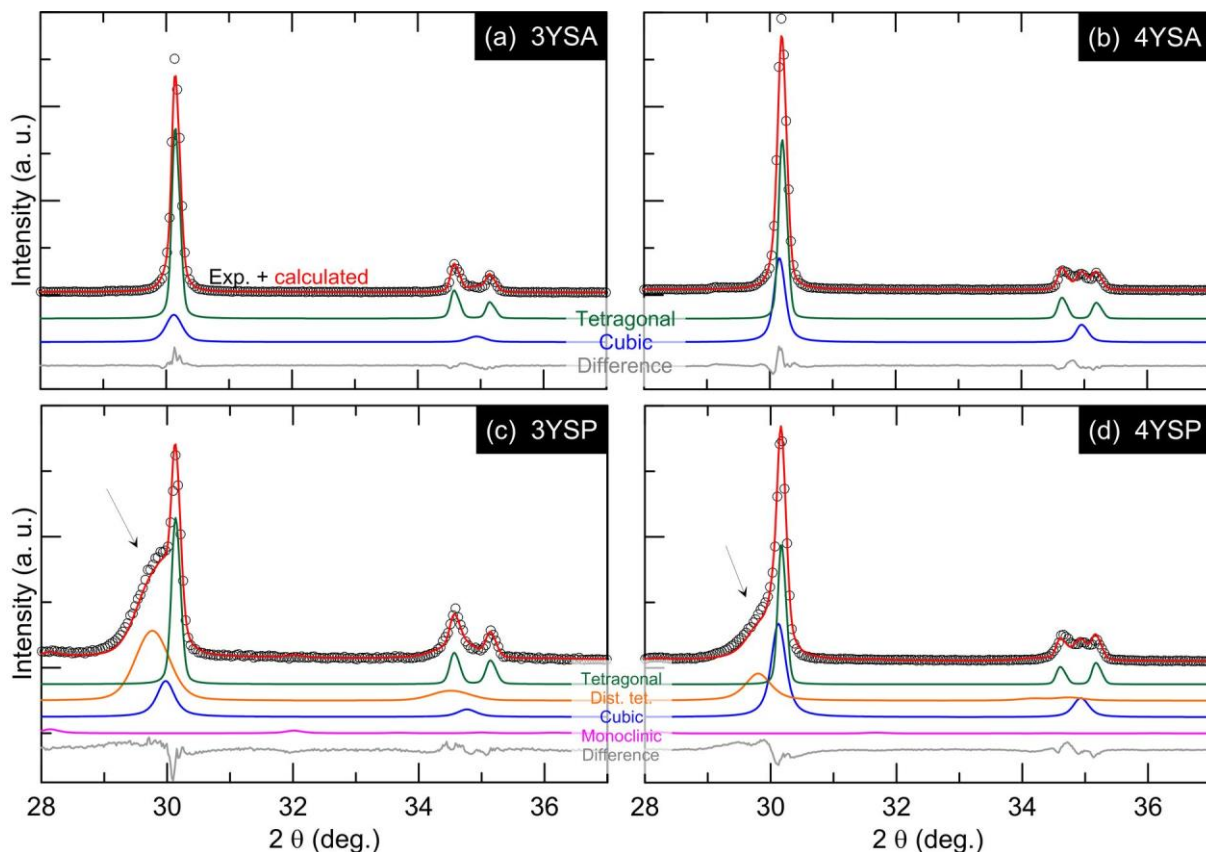


Figure 4: XRD and Rietveld refinement of the different materials

The tetragonal phase was hardly affected by annealing: the crystallite size remains identical (~300 nm for 3YS, ~600 nm for 4YS), the lattice parameters hardly change (a_t undergoes a slight increase (0.02%) while c_t undergoes a slight decrease (-0.01%) for both materials) and a small decrease of the microstress was seen (from ~600 MPa in polished zirconias to ~450 MPa in annealed ones). All these microstructural parameters are summarized in table 2 (it should be kept in mind that these measurements could be conducted on one location of one

sample only for each material, thus their outcomes should be considered as order of magnitudes rather than precise values).

Table 2: structural and microstructural parameters of 3YS and 4YS materials. Numbers written in italic are speculative due to the high convolution of the XRD peaks of the different phases (in particular Cubic and Distorted tetragonal), thus their precision is not known. When possible lattice parameters are written as x.xxxx(y) where y is the precision on the last written digit.

parameter		3YSA	3YSP	4YSA	4YSP
Tetragonal phase	a_t (nm)	0.36044(1)	0.36038(4)	0.36054(1)	0.36043(1)
	c_t (nm)	0.51780(1)	0.51786(4)	0.51782(1)	0.51781(1)
	% Y_2O_3	2.50	2.40	2.70	2.48
	Cryst. Size (nm)	300 (± 20)	290 (± 180)	630 (± 20)	660 (± 250)
	Microstress (σ_{it} , MPa)	460 (± 5)	630 (± 60)	460 (± 20)	580 (± 20)
Distorted tetragonal phase	a_{t-d} (nm)		<i>0.36648</i>		<i>0.36481</i>
	c_{t-d} (nm)		<i>0.51864</i>		<i>0.52450</i>
	Cryst. Size (nm)		<i>67</i>		<i>30</i>
	Microstress (σ_{it} , MPa)		<i>3600</i>		<i>1700</i>
	Stress vs t-phase		<i>2300</i>		<i>2450</i>
Cubic phase	a_c (nm)	0.51291	<i>0.51507</i>	0.51328	<i>0.51328</i>
	Cryst. Size (nm)	<i>67</i>	<i>39</i>	<i>77</i>	<i>52</i>
	Microstress (σ_{it} , MPa)	<i>1200</i>	<i>870</i>	<i>640</i>	<i>750</i>
Weight %	tetragonal	76 (± 0.5)	46 (± 2)	56 (± 2)	35 (± 1)
	Distorted tetragonal	0	25 (± 2)	0	21.5 (± 0.6)
	Cubic	24 (± 0.5)	24 (± 2)	44 (± 2)	42 (± 1)
	Monoclinic	0	5 (± 1)	0	1.5 (± 0.3)

3.2 Ageing of 3Y-TZP

Fig. 5 shows the variation of the surface monoclinic fraction with applied stress on 3YS samples at different ageing time. A high variability in the monoclinic fraction can be seen (error bars are the standard deviation from measurements taken on at least 2 locations on 2 samples). Larger error bars are seen around 0 stress, the location of 0-stress point on the samples are on both extremities, and thus subjected to more positioning error during XRD measurements. Moreover, the control over residual stresses is far from perfect (since they are obtained indirectly by machining and polishing), and this result in increased scattering of the measurements in 3YSP (and later 4YSP) samples.

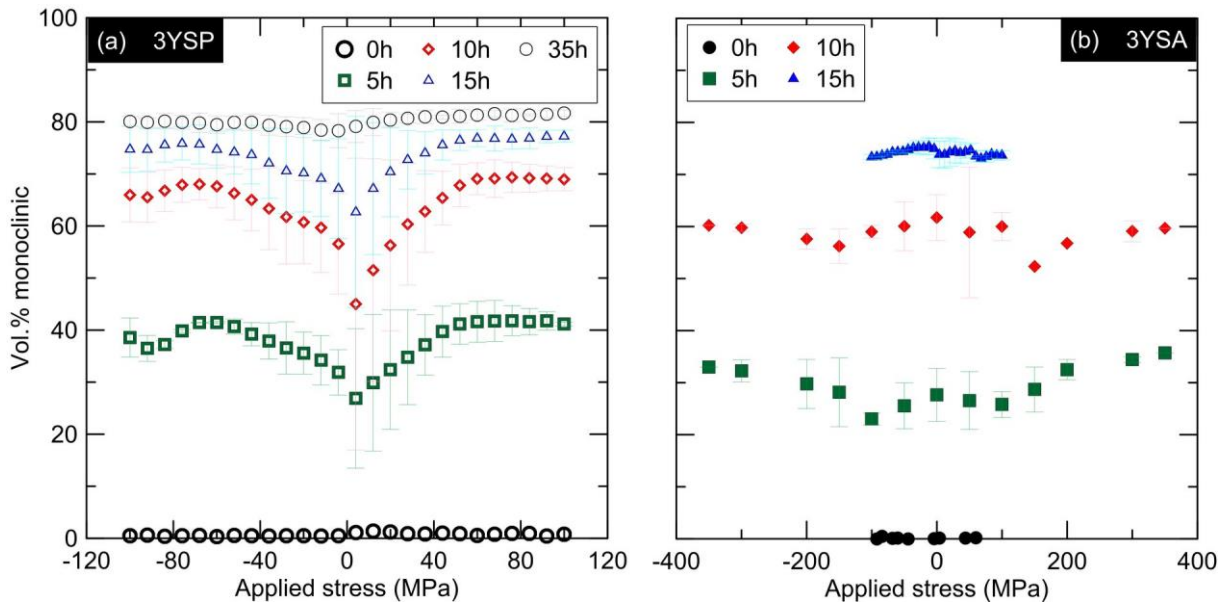


Figure 5: XRD monoclinic fraction measured vs. applied stress on the surface at different ageing time: a. 3YSP; b. 3YSA. Error bars represent the standard deviation of measurements taken on at least two locations on two samples

A comparison between Fig. 5(a) (3YSP) and Fig. 5(b) (3YSA) shows that the residual stresses (generated by machining and polishing) obviously accelerated the ageing process at short ageing times. Moreover, the monoclinic fraction on 3YSP (polished) sample surface increased with increasing stress (both tensile and compressive) even for small applied stresses (less than 60 MPa). The same trend was also present, although less significant for 3YSA (annealed) sample, and it required higher applied stresses (more than 100 MPa). Finally, the effect of applied stresses tends to disappear as hydrothermal ageing progresses: flat V_m -stress profiles are observed for 3YSP after 35 h ageing, and for 3YSA after 10h ageing (even before saturation of the transformation). In addition, the presence of residual or applied stresses doesn't changes the maximum zirconia monoclinic fraction (V_{max}), as can be seen in Fig. 6, but only the ageing rate.

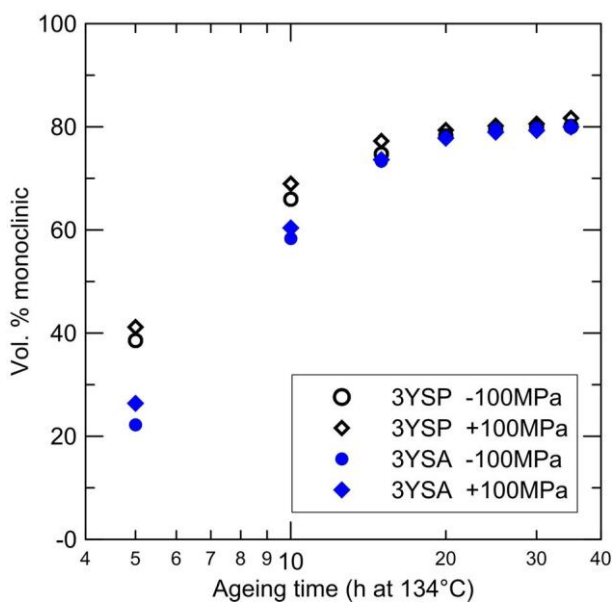


Figure 6: XRD monoclinic fraction measured versus ageing time of 3YS samples

For 3YEA sample (Fig. 7), increasing both compressive and tensile stresses during ageing resulted in increasing slightly the monoclinic fraction. Compared with the 3YS sample, ageing of 3YE is less impacted by applied stress. However, for 3YE samples the effect of applied stresses does not disappear when aging time increases, at least up to 75 h ageing at 134°C.

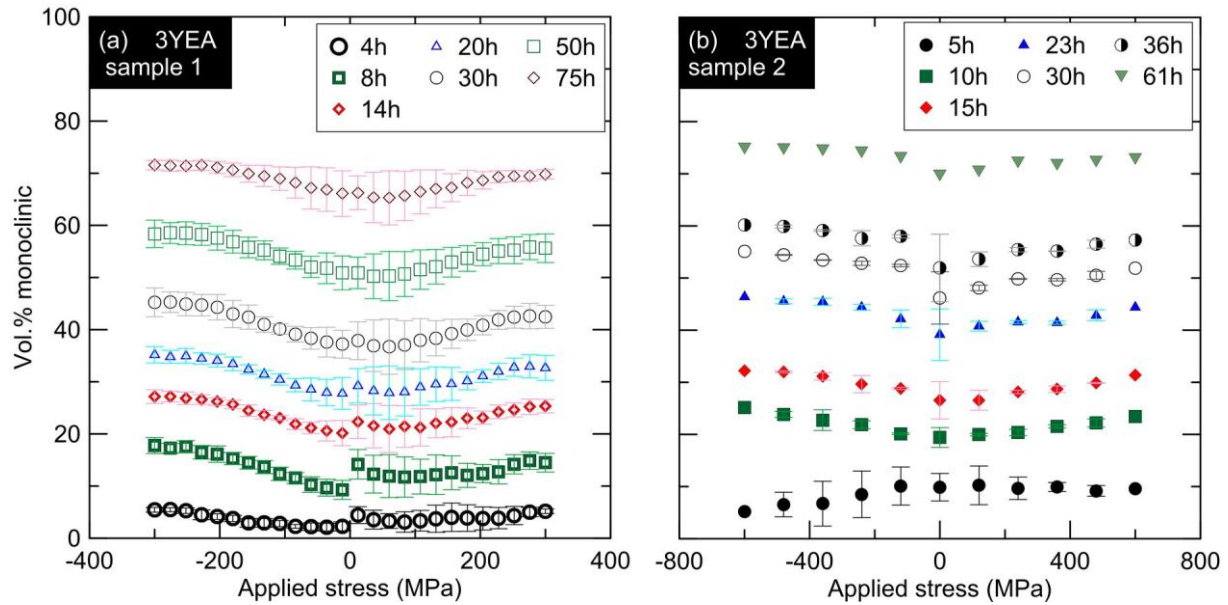


Figure 7: XRD monoclinic fraction measured vs. applied stress on the surface of 3YEA; (a) sample #1; (b) sample #2; when present, error bars represent the standard deviation over 2 measurements on 1 sample

Finally, figures 8 (a) and (c) show the evolution of the XRD diagram of 3YSA and 3YSP during ageing. In particular, for both materials cubic phase remains apparently unaffected by ageing, while both tetragonal and distorted tetragonal phases are transformed to monoclinic during the ageing process. A small decrease of the crystallite size of cubic phase was seen, but can most probably be attributed to a measurement artifact (since both crystallite size and microstress parameters rely on the analysis of the shape (width) of the diffraction peaks, their measurement may also be affected by the “chemical disorder” in the cubic phase and by the presence of cubic grains containing varying amounts of yttrium).

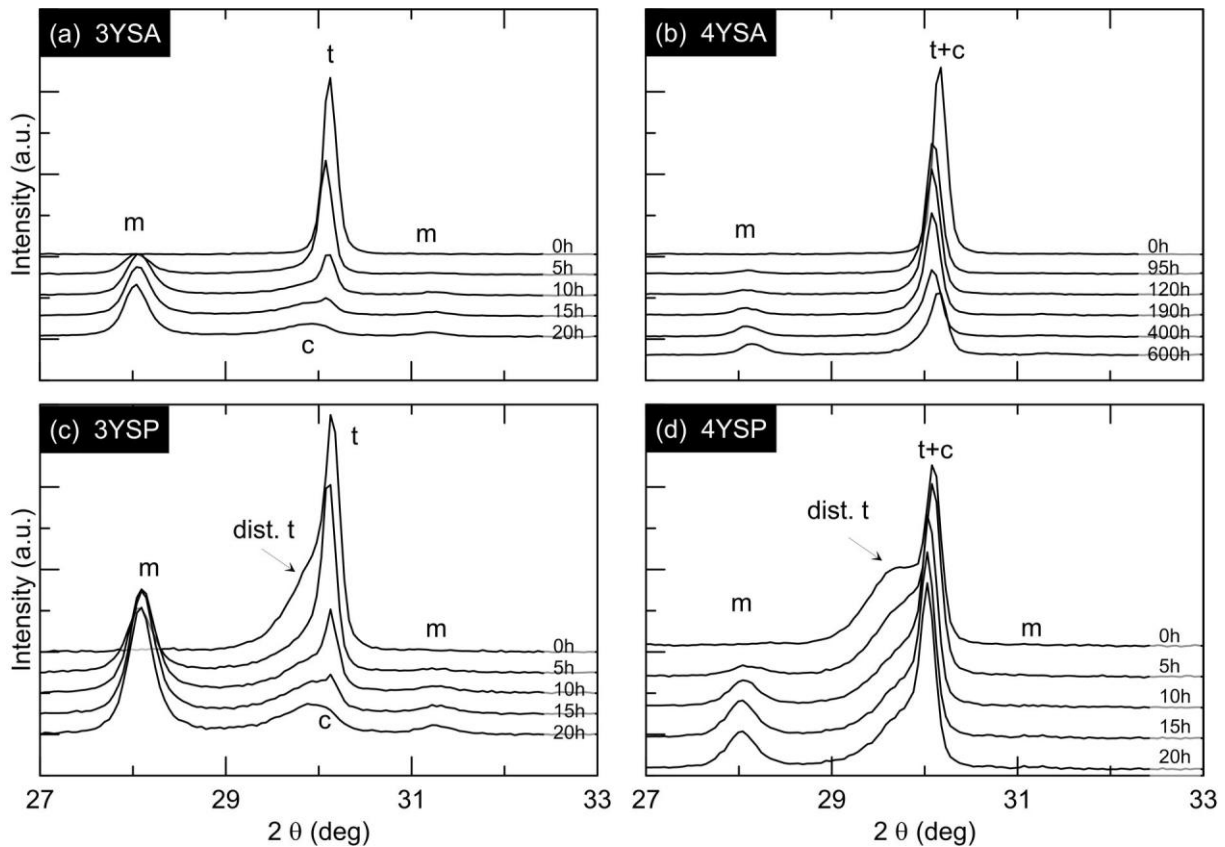


Figure 8: evolution of XRD diagrams of 3YSA (a), 4YSA (b), 3YSP (c) and 4YSP (d) with ageing time at 134°C.

3.3 Ageing of 4Y-TZP

Fig.9 shows the monoclinic fraction measured vs. applied stress on the surface of 4YS-TZP samples at different ageing time. 4YSP samples present a rather similar behavior than 3YSP ones (although longer ageing times are necessary), with tensile and compressive stresses increasing the monoclinic fraction at the beginning of ageing process. However, the large variability makes these evolutions not very statistically relevant. Ageing of 4YSA samples seemed to be the fastest when no stress is applied. It was slower and slower as tensile stresses increased. With increasing compressive stress the transformation rate first decreased then started to increase again for large compressions stresses (lower than -50 MPa), while always staying lower than the transformation rate of the non-loaded material. As can be seen on figure 10, residual stresses (generated by machining and polishing) greatly accelerated the ageing process (the process is about 20 times faster in polished samples than in annealed samples) of 4Y-TZP.

Figure 8 (b) and (d) show that in 4YSP, the distorted tetragonal phase is the first to transform, while the tetragonal phase slowly decreases.

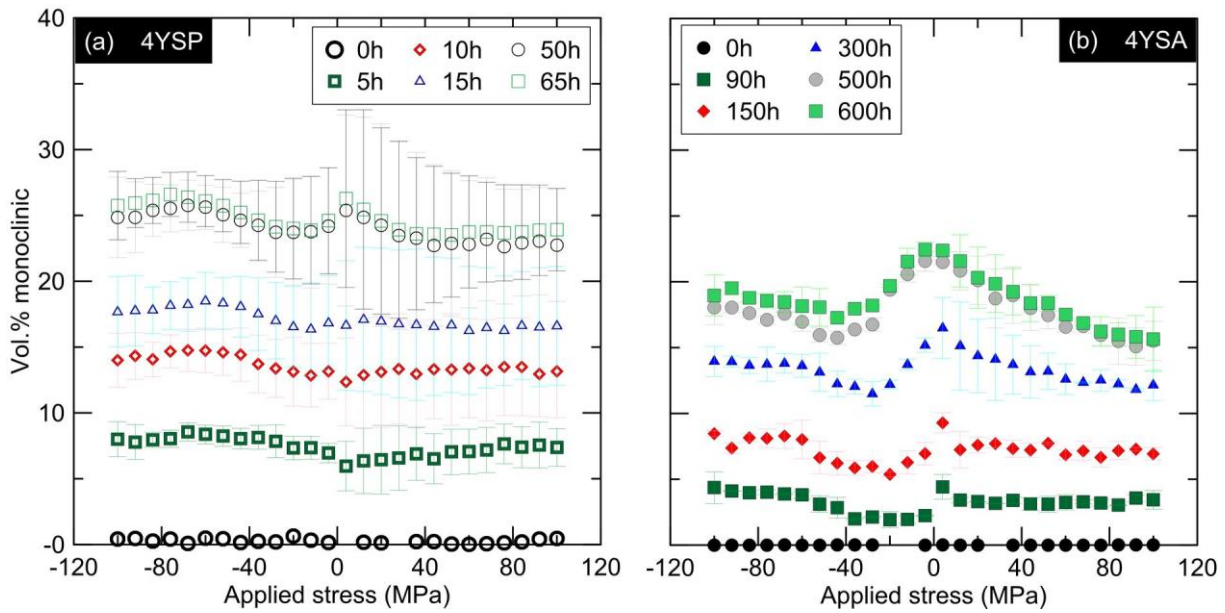


Figure 9: XRD monoclinic fraction measured vs. applied stress on the surface of 4YS-TZP samples. a. 4YSP samples (aged for up to 65h); b. 4YSA (aged for up to 600 h)

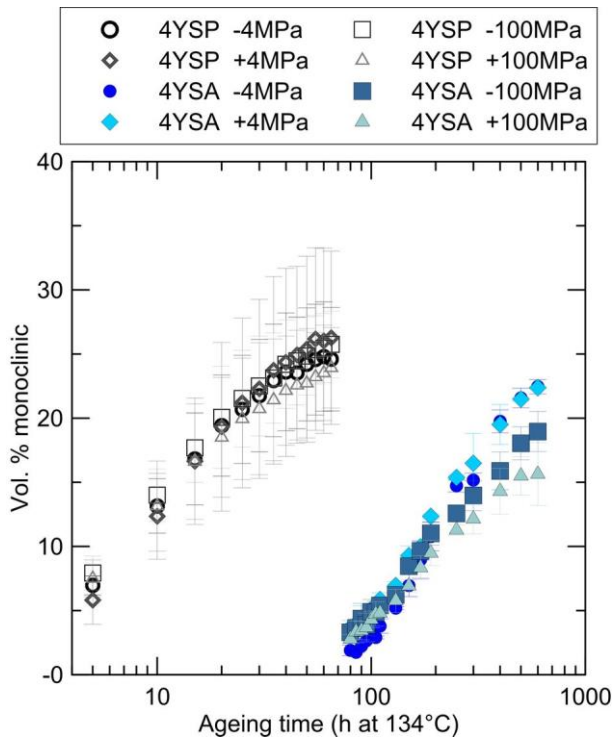


Figure 10: XRD monoclinic fraction measured versus ageing time of 4YS samples

4 Discussions

4.1 Microstructural evolutions with annealing

The microstructural evolutions observed after annealing point to the resorptions of the distorted tetragonal phase and of the monoclinic phase. The small changes in the lattice parameters of tetragonal phases are compatible with small increase of the Y_2O_3 content in tetragonal grains (from 2.4% to 2.5% in 3YS, from 2.5% to 2.7% in 4YS). This is coherent with ZrO_2/Y_2O_3 phase diagram that shows more yttria in the tetragonal phase at 1250°C (annealing temperature) than at 1430°C (sintering temperature). However, this should be considered carefully, since machining and polishing induce large stresses that may affect the

lattice parameters of all phases. Thus the lattice parameter of the stress-free phases of the polished samples is not known, thus the determination of yttria content in the tetragonal phase of polished samples is not precise at all. On plasma-sprayed zirconia, Lipkin *et al.* [17] saw no significant microstructural changes upon annealing with Hollomon–Jaffe parameter [18] lower than or equal to 45 000. In our case, because of the very short annealing time (0.5 h) HJP is around 40 000. As a consequence we chose to consider that annealing does not change the yttria content, thus that the differences between annealed and polished samples mainly come from the presence of residual stresses.

Note that the cubic phase is sometimes seen as yttria-rich tetragonal phase (t'/t'') [19]. Unfortunately, in the present work it was impossible to distinguish between c, t' or t'' phases.

4.2 Macroscopic effect of stresses at long ageing times

At long ageing time, the effect of stresses on ageing seems to disappear. This might be due to two different phenomena. The first one is a measurement artifact related to saturation of the monoclinic fraction: on the one hand, the monoclinic fraction cannot get higher than the initial tetragonal content (if one considers the presence of non-transformable cubic phase); on the other hand, once the volume accessible by XRD is completely transformed, no more evolution of the transformation can be detected by XRD. Thus once saturation is reached, it is obvious that the monoclinic fraction will be independent of applied stress, since it will be at its maximum. The second phenomenon is related to the interplay of residual, applied and t-m transformation-generated stresses [20]: since t-m transformation is accompanied by large volume increase, it gives rise to large stresses that will be superimposed to the existing stress field. Zhang *et al.* [20] found large shifts of the Raman peaks, compatible with tensile stresses, in the tetragonal zone just below the transformed zone. Taking into account the piezospectroscopic coefficients available in the literature [21], these shifts correspond to tensile stresses around 700 MPa, higher than the applied stresses. Thus t-m transformation-generated stresses also influence further ageing, and may become preponderant when the transformed layer is thick enough (Zhang's article deals with transformed depth about 25 μm , whereas we are limited here to 5 μm or less since we hardly reach saturation).

4.3 Effect of stresses on ageing kinetics

In order to understand the influence of applied stress on ageing kinetics of zirconia, all ageing kinetics were fitted using the Mehl–Avrami–Johnson (MAJ) laws (Eq. 4).

$$\frac{V_m - V_0}{V_{max} - V_0} = 1 - \exp(-(bt)^n), \quad b = b_0 \exp\left(-\frac{Q}{RT}\right) \quad (4)$$

where V_m is the monoclinic phase content measured after an exposure of t hours to steam at absolute temperature T , V_0 and V_{max} are the initial and saturation levels of monoclinic phase content, n is an exponent that depends on both nucleation and growth kinetics of the monoclinic phase [10]. b is thermally activated (with Q the activation energy, R the gas constant, and T the absolute temperature). The use of MAJ law derives from the fact that ageing follows a nucleation and growth process. According to previous works, in the MAJ formulation for zirconia ageing the parameter b is proportional to $(N_R \alpha_D^3)^{1/4}$ [10], where α_D is the growth rate of monoclinic spots diameter and N_R is the nucleation rate (if one assumes that the growth rates of monoclinic spot are proportional in diameter and in height, which is the case due to the crystallography of the t-m transformation). The exponent n depends on the ratio between monoclinic phase created during the growth phase and monoclinic phase created during the nucleation phase. If n remains in the [0.5; 2.5] range, it can be

approximated as $n \approx 1 + \frac{3}{4} \log\left(\frac{\alpha_D}{N_R D^2}\right)$ (extrapolated from [11]) (D is the size of the

monoclinic nuclei and can be assimilated to the grain size). Thus for a constant grain size (constant D , as it is the case for a same material submitted to different stress levels) one can deduce schematic evolutions of n and b from those of α_D and N_R :

- 1- If α_D and N_R vary in the same proportions, n remains constant while b varies (b increases if α_D and N_R increase).
- 2- If N_R remains constant and α_D increases, both n and b increase.
- 3- If N_R remains constant and α_D decreases, both n and b decrease.
- 4- If N_R increases and α_D remains constant, b increases and n decreases
- 5- If N_R decreases and α_D remains constant, b decreases and n increases.

Reciprocally, one can deduce the evolutions of α_D and N_R from those of n and b by Eq. (5):

$$\alpha_D = C_\alpha \times b \times 10^{\frac{n-1}{3}} \quad \text{and} \quad N_R = C_N \times b \times 10^{1-n} \quad (5)$$

Here C_α and C_N are constants, and only depend on the material via the grain size. They can be

calculated as: $C_\alpha = \frac{\sqrt{D}}{K}$ and $C_N = \frac{1}{KD^{3/2}}$, with $K = \sqrt[4]{\frac{\pi}{48kl}}$, k being the linear expansion

due to the t-m phase transformation (~1.3%) and l being the depth on which the monoclinic fraction is averaged (~5 μm , if the monoclinic fraction is measured by X-ray diffraction)

Fig.11 shows the evolutions of n and b with applied stress for all materials studied here.

Comparing the polished to annealed samples, both without applied stress, one can infer that residual stress (generated by machining and polishing) can reduce n and increase b , especially for 4YS, which results in accelerated ageing. This is compatible with a higher nucleation rate and a constant growth rate, as in case 4 above. Thus the presence of residual stresses would increase the nucleation rate.

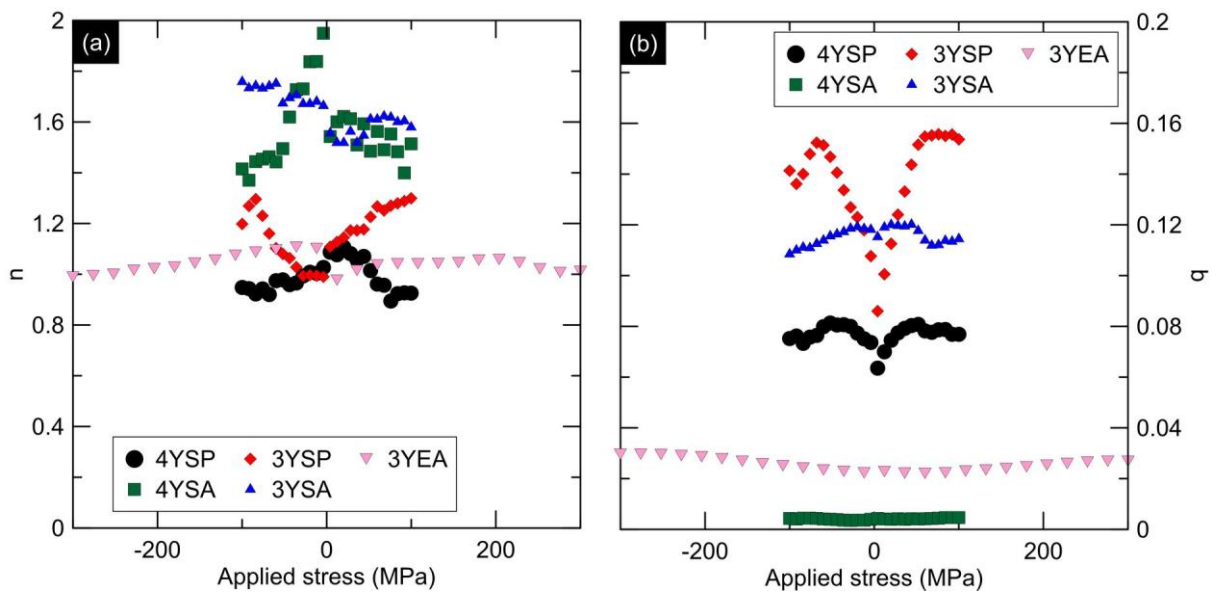


Figure 11: n , b in the MAJ equation for Y-TZP samples vs. applied stress. (a) shows the parameter n , (b) shows the parameter b

In the annealed samples, applied tensile stress has no significant effect on the value of n , but increases the value of b . This indicates a constant nucleation / growth ratio, but an overall faster transformation rate: similarly to case 1 above, tensile stresses seem to increase the nucleation and growth rates by the same ratio. Still in the annealed samples, applied compressive stress can increase the value of n relative to the tensile stress, while b remains in

all cases approximately constant. However, for different materials, the value of n and b show different variation as the compressive stress increases. For 4YSA, n decreases with the increase of compressive stress, while b remains constant around 0.004. For 3YSA, n first increases and then decreases with the increase of compressive stress, and b is fluctuating between 0.115 ± 0.003 with varying compressive stress. For 3YEA, n is fluctuating around 1.0 ± 0.1 with varying applied stress (at ~ 50 MPa (compressive stress) n is slightly higher than for other applied stresses), while b increases with increasing applied stress.

Fig.12 shows the evolutions of α_D and N_R with applied stress for all materials studied. For 4YS samples, residual stresses (generated by machining and polishing) greatly increase the nucleation rate and growth rate, and their nucleation rate increases with the increase of loading stress, while their growth rates have been fluctuating respectively at 0.057 ± 0.003 (polished sample) and 0.0048 ± 0.0004 (annealed sample) being mostly independent on applied stresses. For 3YS samples, residual stresses greatly increase the nucleation rate, but reduce the growth rate. In 3YSA sample, tensile stress (≤ 100 MPa) increases the nucleation rate more than the compressive stress, but compressive stress increases the growth rate more than tensile stress. For 3YE samples, tensile stress increases the nucleation rate more than the compressive stress, and the growth rate is fluctuating around 0.018 ± 0.0015 with varying applied stress.

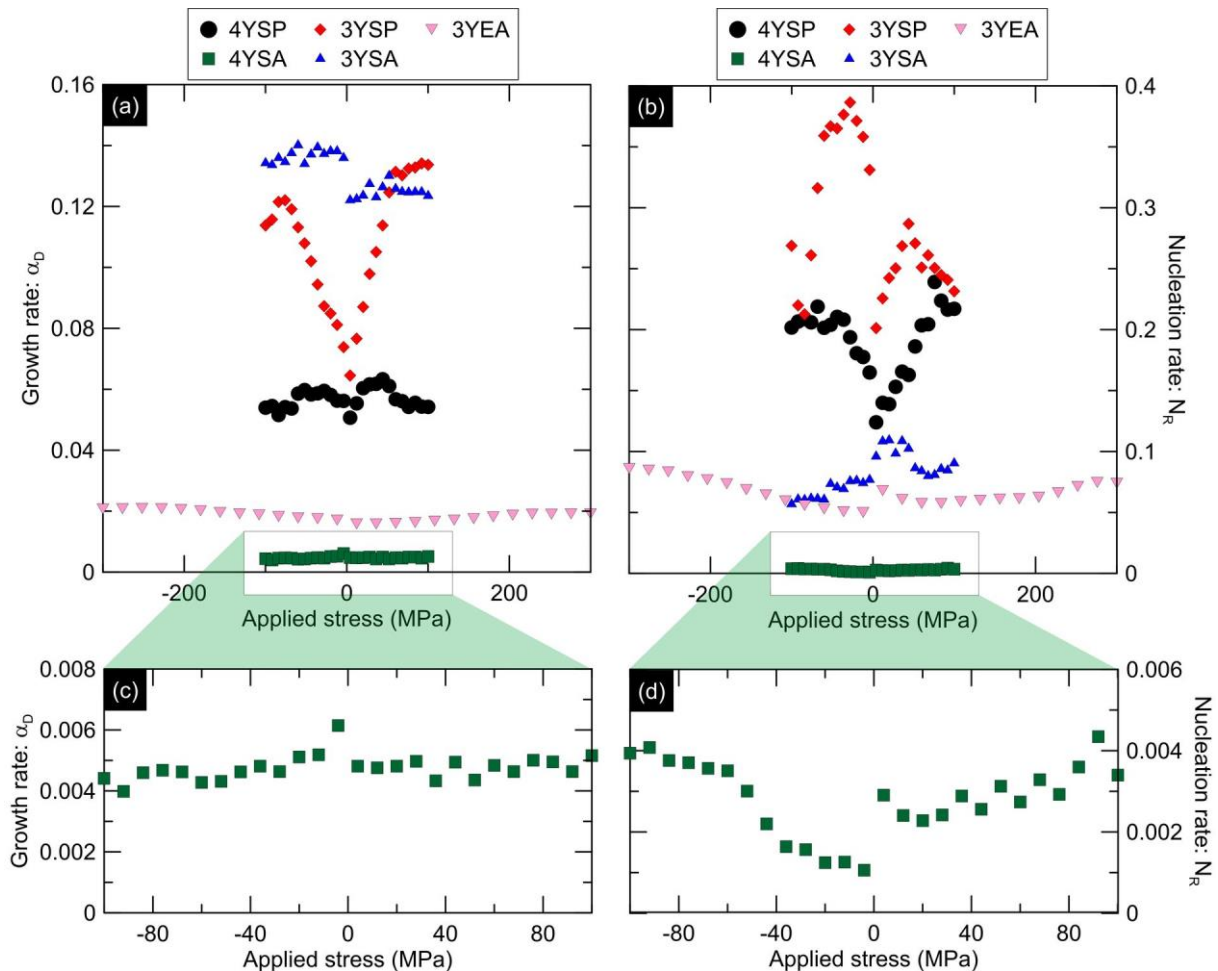


Figure 12: α_D and N_R for Y-TZP samples vs. applied stress.

To understand the great sensitivity of the ageing behavior of 4YS samples to annealing, one might consider the effect of cubic phase. It has been shown that what is called cubic in the present work could in fact be t' or t'' phase, whose coefficient of thermal expansion may vary greatly with the amount of yttrium in their lattice [19]. Here, both the fraction of so-called cubic phase and the amount of yttrium in the cubic phase are higher in 4YS than in 3YS. Thus the fraction of residual stresses due to the presence of the so-called cubic phase might be very different in 3YS and 4YS, hence the higher sensitivity of 4YS to annealing. Finally, one could explain the effect of applied stresses by the mechanism schematized in figure 13. In our samples, there is no deformation when no external stress is applied. This means that residual stresses are in fact second-order stresses and should be perceived as the result of a distribution of microstrain (at the grain-size scale). High residual stresses (such as the ones obtained in polished samples, where tensile stresses higher than a GPa and large microstress were measured, see table 2) correspond to a large distribution, while low residual stresses correspond to a narrower distribution. t - m phase transformation is sometimes described as being triggered when the local stress is higher than a critical stress σ_c^m [22]. With a large stress distribution, the probability that the residual stress locally exceeds σ_c^m is high. It is even higher if an applied stress is superimposed to the stress distribution. Figure 13(a) shows this effect: the continuous curve represents the residual stresses, that exceeds twice σ_c^m (full disks) while the dashed line represents the same residual stresses with a superimposed, constant stress, and exceeds 10 times σ_c^m . On the other hand, when the residual stress distribution is narrow, it may never exceed σ_c^m even in the presence of the same superimposed applied stresses (figure 13 (b)). This explains why increasing stress can lead to increased nucleation and growth rates in polished samples but not in annealed samples (or at a lower degree).

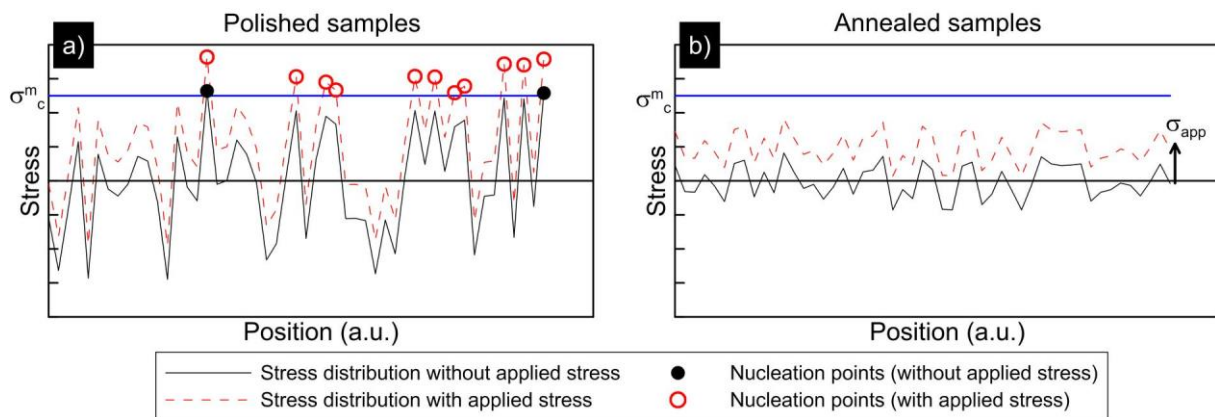


Figure 13: schematic effect of stresses on nucleation of monoclinic phase

Because the thermal activation energy of the combination of aluminum and vacancy ($Al/Y/Zr-V_{\delta}$) is higher than $Y/Zr-V_{\delta}$ [23,24], 3YE samples have a higher resistance to applied stress due to the doping of alumina than other samples during ageing process. 4YS samples, containing more stabilizing ions (Y) than 3YS samples, have a greater number of the oxygen vacancies structures with low thermal activation energy ($Y/Zr-V_{\delta}$), which in turn leads to a higher sensitivity to stress, or rather to mechanical energy brought by stress, than other samples.

5. Conclusion

The effect of stresses on hydrothermal ageing kinetics of zirconia should be examined considering three types of stresses: residual stresses (here tensile stresses due to machining and polishing, reaching the GPa as an order of magnitude, and microstresses), applied stresses (here between -600 and +600MPa, applied by a three points bending test apparatus), and t-m transformation-generated stresses. In general, transformation-generated stresses and residual stresses are larger than applied stresses. However the effect of applied stresses was quite measurable: an acceleration of ageing with applied stress (both tensile and compressive) was observed. The effect of residual stresses was also obvious in 4YS samples: annealing these samples resulted in strongly decreasing residual stresses and strongly slowing the ageing process.

Acknowledgments

C. Wei was supported by a grant from the Chinese Science Council.

References

- [1] J. Chevalier, What future for zirconia as a biomaterial? *Biomaterials*, 27 (2006) 535-543
- [2] S. Schmauder, H. Schubert, Significance of internal stresses for the martensitic transformation in yttria-stabilized tetragonal zirconia polycrystals during degradation, *J. Am. Ceram. Soc.*, 69 (1986) 534-540
- [3] H. Schubert, F. Frey, Stability of Y-TZP during hydrothermal treatment: neutron experiments and stability considerations, *J. Eur. Ceram. Soc.* 25 (2005) 1597–1602
- [4] A. Gebressilassie, Atomic Scale Simulations in Zirconia: Effect of yttria doping and environment on stability of phases, Ph.D. Thesis, INSA-Lyon, France, 2016
- [5] J. Li, L. Zhang, Q. Shen, T. Hashida, Degradation of yttria stabilized zirconia at 370 K under a low applied stress, *Mater. Sci. Eng.*, 297 (2001) 26-30
- [6] V. Lughi, V. Sergo, Low temperature degradation ageing of zirconia: a critical review of the relevant aspects in dentistry, *Dent. Mater.*, 26 (2010) 807-820
- [7] S. Deville, J. Chevalier, L. Gremillard, Influence of surface finish and residual stresses on the ageing sensitivity of biomedical grade zirconia, *Biomaterials*, 27 (2006) 2186-2192
- [8] S. Deville, G. Guenin, J. Chevalier. Martensitic transformation in zirconia-Part I. Nanometer scale prediction and measurement of transformation induced relief, *Acta. Mater.*, 52 (2004) 5697-5707
- [9] S. Deville, G. Guenin, J. Chevalier, Martensitic transformation in zirconia: Part II. Martensite growth. *Acta. Mater.*, 52 (2004) 5709-5721
- [10] J. Chevalier, B. Cales, J.M. Drouin, Low-Temperature Ageing of Y-TZP Ceramics, *J. Am. Ceram. Soc.*, 82 (1999) 2150-2154
- [11] L. Gremillard, J. Chevalier, T. Epicier, S. Deville, G. Fantozzi, Modeling the ageing kinetics of zirconia ceramics, *J. Eur. Ceram. Soc.*, 24 (2004) 3483-3489
- [12] J. Chevalier, C. Olagnon, G. Fantozzi, Study of the residual stress field around Vickers indentations in a 3Y-TZP, *J. Mater. Sci.*, 31 (1996) 2711-2717
- [13] Roa, J. J., Turon-vinas, M., & Anglada, M. Surface grain size and texture after annealing ground zirconia. *Journal of the European Ceramic Society*, 36(6) (2016) 1519–1525.
- [14] H. G. Scott. Phase relationships in the zirconia-yttria system. *J. Mater. Sci.* 10 (1975) 1527
- [15] H. Toraya, M. Yoshimura, S. Somiya, Calibration curve for quantitative analysis of the monoclinic tetragonal ZrO₂ system by X-rays diffraction, *J. Am. Ceram. Soc.*, 67 (1984) 119-121

- [16] R.C. Garvie, P.S. Nicholson, Phase analysis in Zirconia systems, *J. Am. Ceram. Soc.*, 55 (1972) 303-305
- [17] D.M. Lipkin, J. Krogstad, Y. Gao, C. Johnson, W. Nelson, C.G. Levi, Phase Evolution upon Aging of Air-Plasma Sprayed t'-Zirconia Coatings: I-Synchrotron X-Ray Diffraction. *J. Am. Ceram. Soc.*, 96(1) (2013) 290–298
- [18] J. H. Hollomon, L. D. Jaffe, Time-Temperature Relations in Tempering Steel, *Trans. AIME, Iron Steel Div.*, 162 (1945) 223–49
- [19] D. Bucevac, T. Kosmac, A. Kocjan, The influence of yttrium-segregation-dependent phase partitioning and residual stresses on the aging and fracture behaviour of 3Y-TZP ceramics, *Acta Biomaterialia* (2017), <http://dx.doi.org/10.1016/j.actbio.2017.08.014>
- [20] F. Zhang, M. Inokoshi, K. Vanmeensel, B; Van Meerbeek, I. Naert, J. Vleugels, Lifetime estimation of zirconia ceramics by linear ageing kinetics, *Acta Materialia* 92 (2015) 290-298
- [21] G. Pezzotti, A.A. Porporati, Raman spectroscopic analysis of phase-transformation and stress patterns in zirconia hip joints, *Journal of Biomedical Optics*, 9 (2004) 372
- [22] R.M. McMeeking et E.G. Evans, Mechanics of transformation toughening in brittle materials, *J. Am. Ceram. Soc.* 65 (1982) 242-46
- [23] X. Guo, R. Waser, Electrical properties of the grain boundaries of oxygen ion conductors: Acceptor-doped zirconia and ceria, *Prog. Mater. Sci.*, 51 (2006) 151-210
- [24] A. Samodurova, A. Kocjan, M.V. Swain, T. Kosmac, The combined effect of alumina and silica co-doping on the ageing resistance of 3Y-TZP bioceramics, *Acta Biomater.*, 11 (2015) 477-487